

Diminished Chondrogenesis and Enhanced Osteoclastogenesis in Leptin-Deficient Diabetic Mice (*ob/ob*) Impair Pathologic, Trauma-Induced Heterotopic Ossification

Shailesh Agarwal, Shawn Loder, John Li, Cameron Brownley,
Jonathan R. Peterson, Eboda Oluwatobi, James Drake, David Cholok,
Kavitha Ranganathan, Hsiao Hsin Sung, James Goulet,
Shuli Li, and Benjamin Levi

Diabetic trauma patients exhibit delayed postsurgical wound, bony healing, and dysregulated bone development. However, the impact of diabetes on the pathologic development of ectopic bone or heterotopic ossification (HO) following trauma is unknown. In this study, we use leptin-deficient mice as a model for type 2 diabetes to understand how post-traumatic HO development may be affected by this disease process. Male leptin-deficient (*ob/ob*) or wild-type (C57BL/6 background) mice aged 6–8 weeks underwent 30% total body surface area burn injury with left hind limb Achilles tenotomy. Micro-CT (μ CT) imaging showed significantly lower HO volumes in diabetic mice compared with wild-type controls (0.70 vs. 7.02 mm³, $P < 0.01$) 9 weeks after trauma. *Ob/ob* mice showed evidence of HO resorption between weeks 5 and 9. Quantitative real time PCR (qRT-PCR) demonstrated high *Vegfa* levels in *ob/ob* mice, which was followed by disorganized vessel growth at 7 weeks. We noted diminished chondrogenic gene expression (SOX9) and diminished cartilage formation at 5 days and 3 weeks, respectively. Tartrate-resistant acid phosphatase stain showed increased osteoclast presence in normal native bone and pathologic ectopic bone in *ob/ob* mice. Our findings suggest that early diminished HO in *ob/ob* mice is related to diminished chondrogenic differentiation, while later bone resorption is related to osteoclast presence.

Introduction

RECOVERY FROM TRAUMA is a tightly regulated process requiring specific local and systemic signals to restore normal form and function. Disruption or dysregulation at any stage leads to a range of pathologic states. Heterotopic ossification (HO) is a disorder of wound healing characterized by the anomalous development of ectopic bone in the extra-skeletal tissue [1–3]. Patients at risk for HO development include those with pressure ulcers, trauma, burns, spinal cord/brain injury, joint replacements, and long bone fractures. In these patients, HO may result in limited range of motion, nerve entrapment, chronic pain, and nonhealing wounds. Despite its prevalence among patients with severe trauma, effective treatment strategies addressing the growth of ectopic bone remain elusive.

Similar to normal fracture healing, HO is believed to develop through an endochondral intermediary [4,5]. Metabolic derangements, including diabetes, can result in decreased

bone mineral density and impaired fracture site healing in normal bone [6–8]. Leptin-deficient mice, which exhibit hyperglycemia and obesity similar to patients with type 2 diabetes, are known to exhibit diminished bone volume and osteoporosis [9,10]. Mesenchymal stem cells (MSCs) cultured in the presence of high-glucose exhibit diminished chondrogenesis [11]. Additionally, osteoclast upregulation may contribute to bone turnover in diabetic patients [12,13]. Understanding how diabetes affects HO could elucidate new strategies for inhibiting or limiting this debilitating condition.

We have previously described a mouse model of HO using a systemic 30% total body surface area (TBSA) partial-thickness burn with Achilles tenotomy of the hind limb [14]. Wild-type mice (C57BL/6) develop heterotopic cartilage within 3 weeks post-trauma and undergo endochondral ossification by 5 weeks. In this study, we investigate the impact of leptin deficiency, as a model of type 2 diabetes, on heterotopic bone formation using our in vivo mouse model of burn with tenotomy in *ob/ob* and wild-type

mice and our in vitro model of adipose-derived mesenchymal stem cell (adMSC) culture [14].

Materials and Methods

Mice

Animal procedures were carried out in accordance with guidelines from the *Guide for the Use and Care of Laboratory Animals: Eighth Edition*, approved by the Institutional Animal Care and University Committee on the Use and Care of Animals of the University of Michigan (UCUCA PRO0001553). Young (10–12 weeks), male, leptin-deficient diabetic mice (*ob/ob*) [15,16] on a C57BL/6 background and wild-type C57BL/6 mice purchased from Jackson Laboratory were used for all experiments. Mice were housed three per cage at 72F (\pm 4F) with 12 h of light exposure daily (325 lux) and fed 5LOD chow.

Burn injury and tenotomy

All mice intended for in vivo development of HO underwent 30% TBSA partial-thickness burn injury to the dorsum under 3% inhaled isoflurane [2]. A metal block was heated to 60°C in a water bath and placed over the shaved dorsum for 18 s. Following burn injury, mice received a left hind limb Achilles tenotomy using sterile surgical scissors, and the incision was closed with a single 5-0 vicryl suture. Animals were housed in UCUCA-supervised facilities, three per cage, receiving 12 h of light exposure daily, with no restrictions to diet. All mice were housed in the same facility.

Osteogenic differentiation of adMSCs

Ob/ob and wild-type mice were prepared for harvest of adMSCs [17]. Mice underwent 30% TBSA burn *without* tenotomy or no burn injury at all. After 2 h, mice were euthanized and adMSCs were harvested from the bilateral inguinal regions. AdMSCs were chosen as a proxy for the still unidentified mesenchymal cell responsible for HO formation [14] and have shown capacity for bone formation in vivo and in vitro [2].

MSCs were seeded in triplicate onto 6- and 12-well plates and cultured in the osteogenic differentiation medium (DMEM with 10% FBS, 1% penicillin/streptomycin, 10 mM β -glycerophosphate, 100 μ g/mL ascorbic acid, Invitrogen). Early osteogenic differentiation was assessed by an alkaline phosphatase (ALP) stain after 7 days [2]. Alizarin red staining for bone mineral deposition was completed at 2 weeks [2].

μ CT imaging and analysis

In vivo development of HO was assessed with longitudinal μ CT scans at 5, 7, and 9 weeks after trauma for each mouse ($n=3$ for *ob/ob* and for wt/wt mice) (μ CT: GE Healthcare Biosciences, using 80 kVp, 80 mA, and 1,100 ms exposure). Images were reconstructed and HO volume was computed using a calibrated imaging protocol [18]. Heterotopic bone was calculated between Hounsfield units of 1,250 and 1,800. The voxel size for all scans is 48.08 μ m, and the field of view is 38.47 \times 38.47 cm. Scans were performed from the most distal aspect of the foot to the mid-thigh. The region of interest evaluated for HO extended from the knee to the foot.

MICROFIL imaging and analysis

In vivo collateral vessel formation was assessed using MICROFIL [19]. At week 7, *ob/ob* and wild-type mice ($n=3$ each) were euthanized and perfused through the descending thoracic aorta MICROFIL (MV120-blue; Flow Tech Inc.) until it flowed out through the vented inferior vena cava. MICROFIL was allowed to polymerize overnight at 4°C within the vasculature. μ CT imaging was performed to assess vasculature. Total MICROFIL volume was computed using a calibrated imaging protocol [20].

Histology

Before injury, or at 5 days ($n=2$), 3 weeks ($n=2$), and 3 months ($n=5$) after burn injury/tenotomy, animals were euthanized and the tenotomized legs from mid-thigh onward were fixed, decalcified in 19% EDTA, paraffin embedded, and sectioned at 5 μ m. Slides were stained with penta-chrome for cartilage and ectopic bone and Tartrate-resistant acid phosphatase (TRAP) for osteoclast presence [14,21]. Immunohistochemical staining was performed with the following primary antibodies at 1:100 dilutions: anti-HIF-1 α , anti-VEGF-A, anti-SOX9, and anti-CD31.

RNA collection and qRT-PCR from histologic slides

Histologic sections of the left hind limbs from burned *ob/ob* and wild-type mice were collected 5 days post-trauma ($n=2$). Additionally, the histologic section of the left hind limb from uninjured unburned *ob/ob* and wild-type mice was also collected. Local soft tissue at the tenotomy site posterior to tibia/fibula was isolated at 20 \times magnification and digested in Proteinase K, followed by QIAzol lysis buffer (Qiagen) and chloroform extraction. mRNA was treated with DNase Turbo (ThermoFisher Scientific) and reverse transcribed to cDNA using TaqMan Reverse Transcription Reagents (Applied Biosystems). Quantitative real time PCR was completed using SYBR Green PCR Master Mix (Applied Biosystems). Specific primers for these genes corresponded to their PrimerBank sequences. Transcript levels were standardized to internal *gapdh* transcript levels. All reactions were run in triplicate.

Statistical analysis

Data were analyzed using SPSS software (v21, IBM). Means and standard deviations were calculated, and statistical analysis was performed using Student's *t*-test. In figures, bar graphs represent means, whereas error bars represent one standard deviation. For all assays, significance was defined as $P < 0.05$.

Results

Ob/ob mice produce significantly less HO after injury

μ CT imaging was performed at 5–9 weeks after injury to quantify total HO volume. The HO volume in *ob/ob* mice was significantly lower than wild-type mice at each time point with the greatest difference existing at 9 weeks. At 9 weeks, the HO volume in *ob/ob* mice was 0.70 mm³ (SD 0.23 mm³) versus 7.02 mm³ (SD 1.42) in wild-type mice ($P < 0.01$) (Fig. 1A, B).

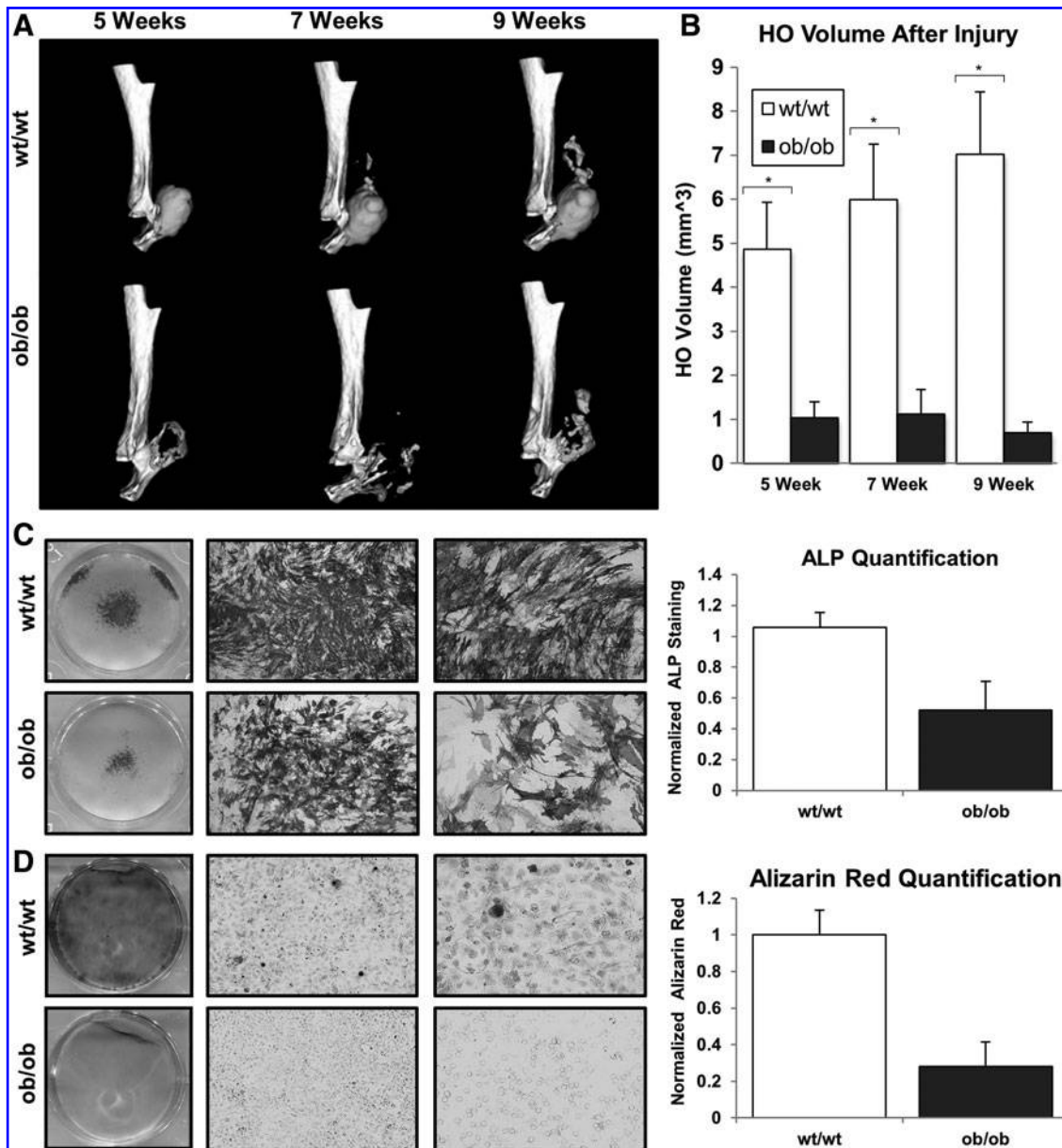


FIG. 1. (A) Micro-CT imaging of representative *ob/ob* and wild-type hind limbs at 5, 7, and 9 weeks post-trauma. Areas of HO are indicated in gray. (B) Total quantified HO volume at 5, 7, and 9 weeks post-trauma in *ob/ob* and wild-type mice (* $P < 0.05$). (C) Alkaline phosphatase staining of adipose-derived mesenchymal stem cells (adMSCs) from burned *ob/ob* and wild-type mice at 7 days. (D) Alizarin red staining of adMSCs from burned *ob/ob* and wild-type mice at 14 days. HO, heterotopic ossification.

AdMSCs were harvested from *ob/ob* and wild-type mice 2 h after burn injury. Both ALP and alizarin red staining confirmed significantly diminished osteogenic differentiation of adMSCs from burned *ob/ob* mice at 7 and 14 days after initiation of osteogenic culture, respectively (Fig. 1C, D). Similarly, we noted that unburned wild-type adMSCs were more osteogenic with respect to ALP expression compared with *ob/ob* adMSCs (Supplementary Fig. S1; Supplementary Data are available online at www.liebertpub.com/scd). Interestingly, we found that while burn injury has been reported to increase osteogenic differentiation of adMSCs from wild-type mice, the opposite was true of adMSCs from *ob/ob* mice, which decreased in osteogenic

differentiation upon burn injury (Fig. 1 and Supplementary Fig. S1).

Ob/ob exhibit evidence of hyperglycemia and hyperinsulinemia

To confirm that the *ob/ob* mice in our study approximated type 2 diabetes, we assessed serum glucose and insulin (Supplementary Fig. S2). Using serum analysis of the specific mice in our study, we found that at both 5 days and 3 weeks after injury, the *ob/ob* mice had significantly higher serum glucose levels compared with wild-type mice at the same time points after injury (day 5: 700 mg/dL vs. 281 mg/dL,

$P < 0.05$; week 3: 663 mg/dL vs. 273 mg/dL, $P < 0.05$). Serum insulin levels were also significantly higher in *ob/ob* mice compared with wild-type mice (day 5: $>300 \mu\text{M}/\text{mL}$ vs. $7.3 \mu\text{M}/\text{mL}$, $P < 0.05$; week 3: $>300 \mu\text{M}/\text{mL}$ vs. $10.3 \mu\text{M}/\text{mL}$, $P < 0.05$). Additionally, we found that the hind limbs of *ob/ob* mice weighed significantly more compared with wild-type mice (1.41 g vs. 0.63 g, $P < 0.05$). Finally, we noted that the uninjured right hind limb of *ob/ob* mice exhibited substantially more adipose tissue compared with the uninjured right hind limb of wild-type mice.

Ob/ob mice exhibit more angiogenic signaling at the trauma site compared with wild type

Mean vessel volumes (MVV) in the injured hind limb of burned diabetic and wild-type mice at 7 weeks after injury were compared (Fig. 2A). MVV in diabetic mice were significantly greater than wild type (9.47 mm^3 vs. 3.22 mm^3 , $P < 0.01$). Although difficult to quantitate, the vessels in *ob/ob* mice are narrower and more disorganized.

When adjusting for limb mass, diabetic limbs continued to have increased MVV ($6.87 \text{ mm}^3/\text{g}$ vs. $5.31 \text{ mm}^3/\text{g}$, $P < 0.01$) (Fig. 2B). At 3 weeks, we found more small vessels in diabetic mice based on CD31 staining (Fig. 2C). Upon staining of wild-type and *ob/ob* hind limbs in the absence of burn/tenotomy, we found more CD31+ vessels in wild-type mice suggesting that baseline vessel presence is elevated in uninjured wild-type mice (Supplementary Fig. 3A, B).

At 5 days post-trauma, there was similar staining for *Hif1 α* at the hind limb of diabetic and wild-type mice (Fig. 2D). RNA transcript levels of *Hif1 α* were higher in histologic sections of the diabetic hind limb at the injury site (Fig. 2E). A similar comparison of *Vegfa* levels showed more *Vegfa* staining in the *ob/ob* hind limb, again confirmed based on RNA transcript levels at 5 days post-trauma (Fig. 2F, G). We found elevated *Vegfa* immunostaining in uninjured wild-type mice compared with uninjured *ob/ob* mice, although RNA analysis did not suggest a significant difference (Supplementary Fig. 3C, D).

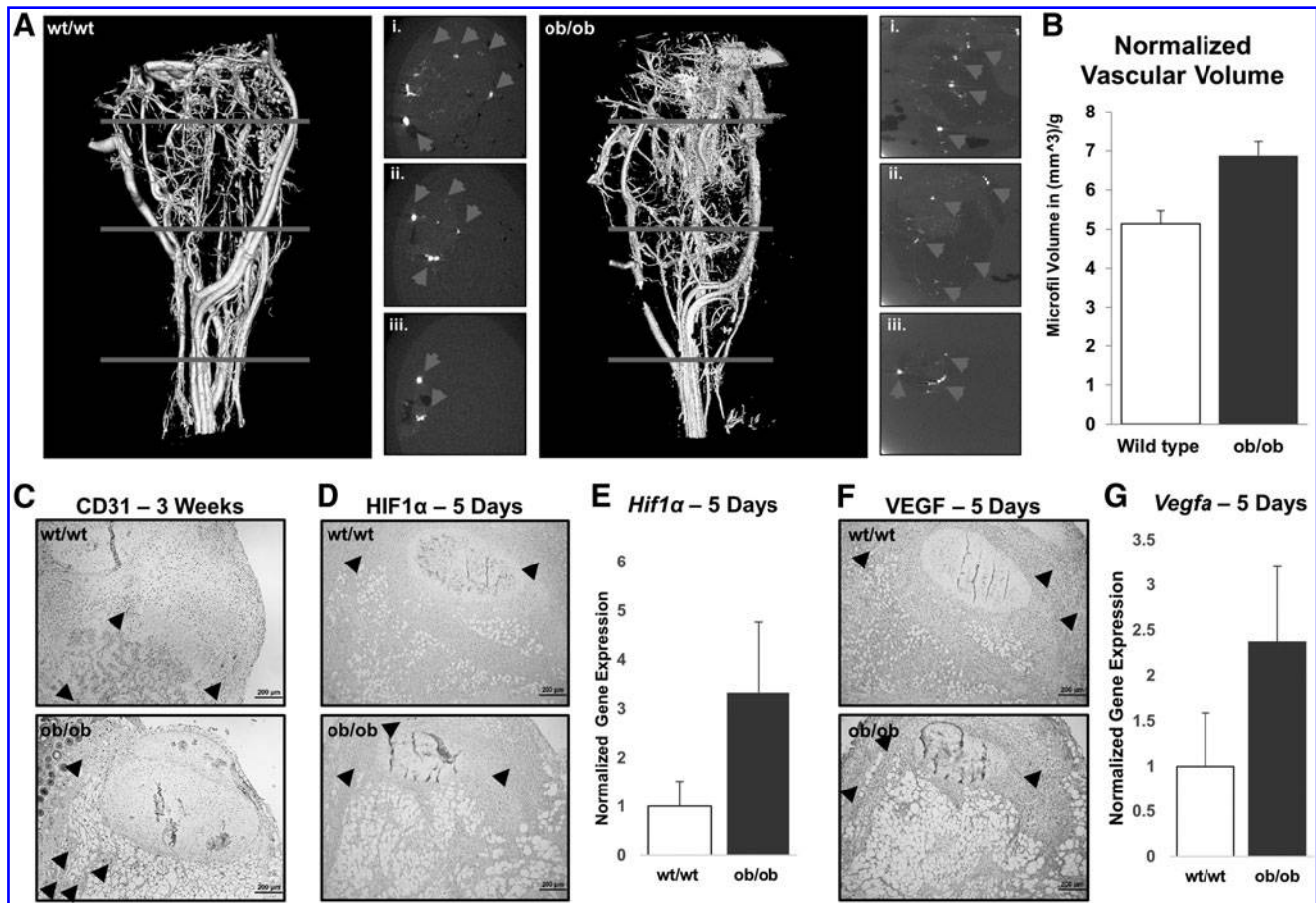
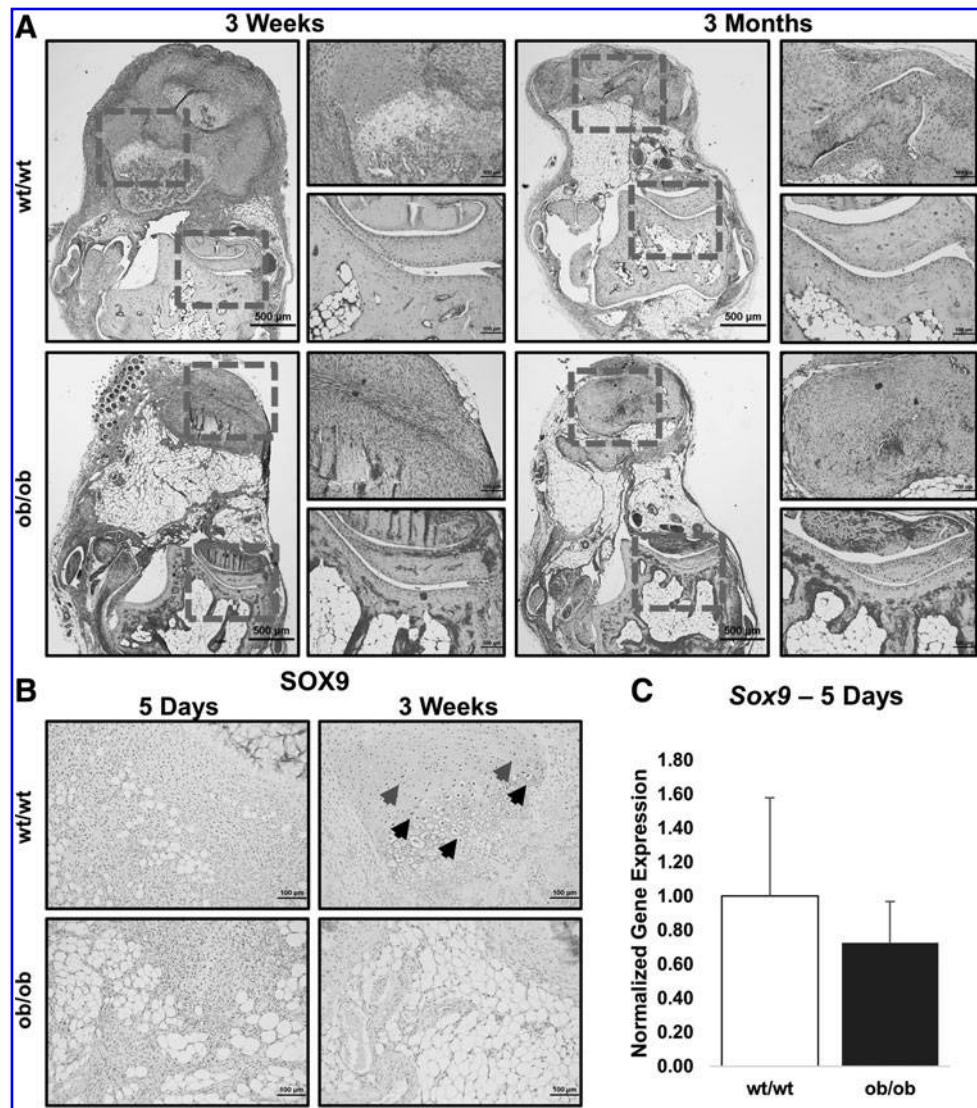


FIG. 2. (A) Vessel reconstruction after MICROFIL injection at 7 weeks of *ob/ob* and wild-type hind limbs depicts more vessel growth with disorganization in *ob/ob* mice. Cross sections taken from the *top* third, *middle* third, and *bottom* third of both legs are depicted to the *right*. Gray arrowheads = MICROFIL dye in vessels. (B) Mean vessel volume standardized to hind limb mass. (C) Staining for CD31 (black arrowheads) shows comparable amount of staining in both *ob/ob* and wild-type hind limbs after 3 weeks. (D) Staining for *Hif1 α* (black arrowheads) is comparable between *ob/ob* and wild-type mice after 5 days. (E) Higher *Hif1 α* RNA transcript level in the diabetic hind limb compared with wild type after 5 days, standardized to internal *Gapdh* levels [normalized ratios 3.33 (SD 1.44) vs. 1.00 (SD 0.52)]. (F) VEGF staining is increased in the *ob/ob* hind limb 5 days postinjury. (G) *Vegfa* RNA transcript levels are higher in the *ob/ob* hind limb after 5 days, standardized to internal *Gapdh* levels [normalized ratios 2.38 (SD 0.83) vs. 1.00 (SD 0.59)]. * $P < 0.05$.



Decreased cartilage formation in *ob/ob* mice at 3 weeks and 3 months postinjury

Despite increased angiogenic signaling based on the RNA transcript level, protein expression, and final vessel growth, pentachrome and SOX9 staining confirmed that *ob/ob* mice exhibit diminished cartilage formation. At the level of tenotomy, we found robust alcian blue staining representative of cartilage after 3 weeks in pentachrome-stained sections of wild-type mice only (Fig. 3A). *Ob/ob* mice exhibited less SOX9 staining compared with wild type at the site of future HO development 3 weeks after injury, coinciding with areas of blue stain in our pentachrome-stained sections (Fig. 3B). RNA analysis did not indicate a significant difference in *Sox9* expression early after trauma, however (Fig. 3C).

Ectopic bone has diminished collagen and osteoblast presence in *ob/ob* mice

Ectopic and normal cortical bone from wild-type and *ob/ob* mice was stained with aniline blue. Both ectopic bone and normal cortical bone from *ob/ob* mice had diminished

osteoid staining compared with respective bone from wild-type mice (Fig. 4). Furthermore, osteoblast presence was diminished within the ectopic bone of *ob/ob* mice compared with wild-type mice by osteocalcin immunofluorescence (Fig. 4).

Ectopic bone resorbs during the initial weeks after injury in *ob/ob* mice

Upon further evaluation of the μ CT images, we noted decreases in HO volume from weeks 5 to 7, and again from weeks 7–9, indicative of bony resorption in *ob/ob* mice (Fig. 5A). HO resorption was not observed in wild-type mice at any time point [14].

Increased osteoclast presence in heterotopic bone from *ob/ob* mice

Tartrate-resistant acid phosphatase (TRAP) staining of *ob/ob* and wild-type mice was performed at 5 days, 3 weeks, and 3 months post-trauma to assess osteoclast presence. While wild-type HO had no evidence of osteoclast activity,

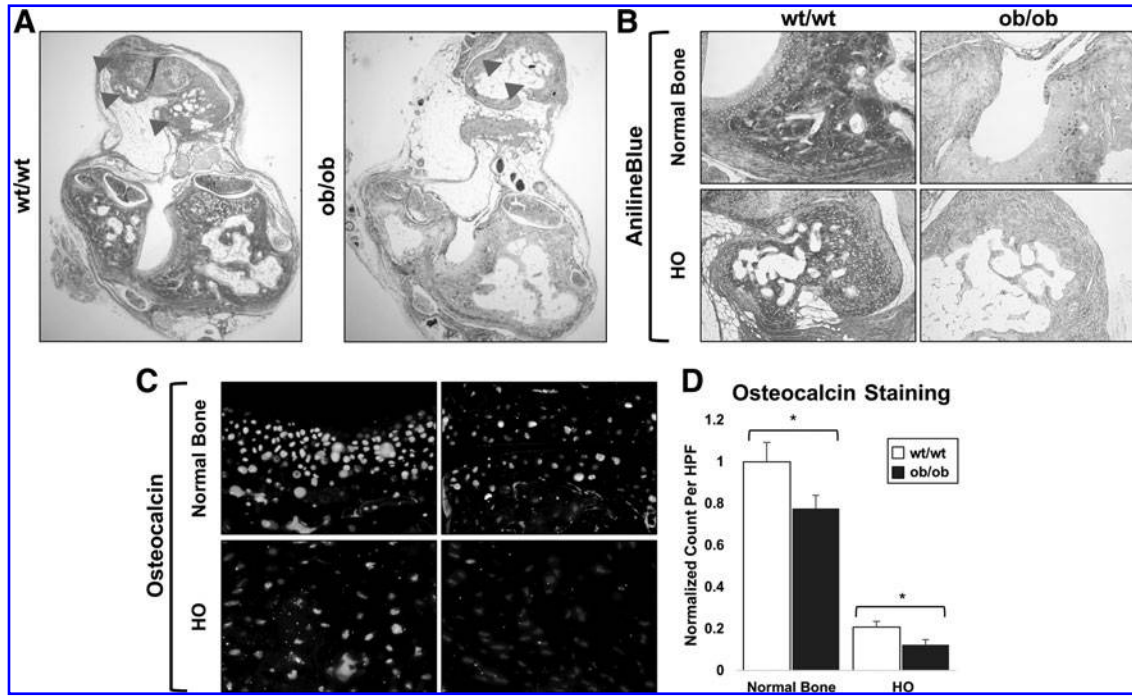


FIG. 4. (A) Aniline blue stain of *wt/wt* and *ob/ob* sections 3 months after injury with regions of HO indicated (gray arrowheads) (4× magnification). (B) Aniline blue stain of normal bone and HO 3 months after injury in *wt/wt* and *ob/ob* mice (10×). (C) Representative osteocalcin immunofluorescent staining in normal bone and HO in *wt/wt* and *ob/ob* mice 3 months after injury (20×). (D) Increased osteocalcin staining per high-powered field in normal bone and HO of *wt/wt* mice compared with *ob/ob* mice ($n=3$ sections for *wt/wt* and *ob/ob* mice).

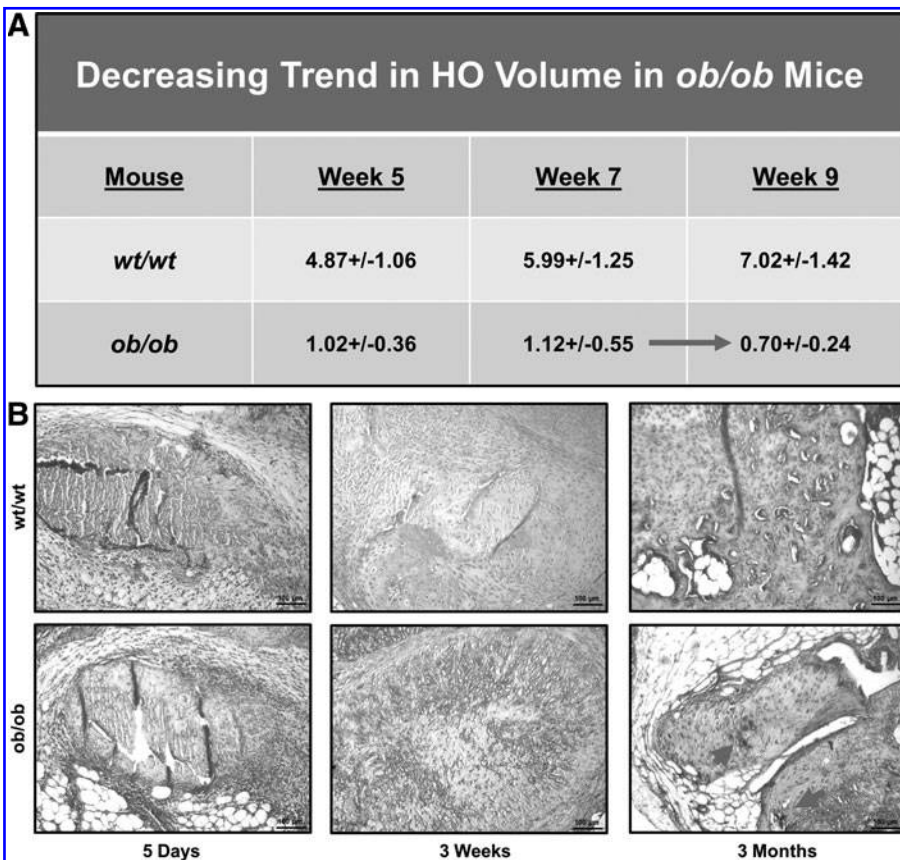


FIG. 5. (A) Decreasing trend in HO volume of *ob/ob* mice over time compared with wild-type mice (gray arrowheads). (B) Increased osteoclast activity based on TRAP staining of *ob/ob* and wild-type HO regions.

we found robust osteoclast presence at the 3-month time point in HO from *ob/ob* mice (Fig. 5B). This osteoclastogenesis is not seen even if wild-type mice are followed out to 15 weeks demonstrating dysregulated bone homeostasis in our *ob/ob* mice.

Discussion

In this study, we use leptin-deficient mice (*ob/ob*) as a model of type 2 diabetes to determine the impact on HO following trauma. HO is a condition characterized by ectopic bony lesions within soft tissues. This condition often develops in patients with severe trauma such as large surface area burns, blast injuries, or surgical procedures. As a result, patients develop chronic pain, open wounds, restricted range of motion at joints, and nerve impingement [1–3]. Our interest in studying HO in the context of a model of type 2 diabetes was driven by previous studies demonstrating increased fracture risk and impaired fracture healing in diabetic patients and animal models, as well as less incidence of HO in diabetes patients [6–8]. No studies have examined the impact of diabetes on the production of pathologic heterotopic bone post-trauma. By identifying the impact of a pathologic metabolic condition on pathologic bone formation, we may begin to identify potential targets to prevent or limit HO in patients.

Our model of post-traumatic HO reliably produces radiographically evident HO as early as 5 weeks after injury in wild-type mice and closely resembles patients at risk for HO—those with large burns and/or significant trauma. By using a leptin-deficient model (*ob/ob*), we focused on a model of diabetes closely resembling the metabolic syndrome experienced by type 2 diabetic patients, which has been shown to closely resemble pathologic wound healing in diabetic patients [22]. Serum glucose and insulin analyses of the mice included in our study confirm that these mice demonstrate some of the components of type 2 diabetes.

We found that *ob/ob* mice produce significantly less HO compared with wild type. Furthermore, HO, which forms initially in the *ob/ob* mouse, slowly resorbs over time. Overall, our study demonstrates that leptin deficiency may limit pathologic bone formation.

In vitro osteogenic differentiation

Our findings indicate that the osteogenic differentiation of adMSCs derived from burned wild-type mice is elevated compared with adMSCs derived from burned *ob/ob* mice. However, our finding that burn injury actually caused a decrease in the osteogenic differentiation of adMSCs from *ob/ob* mice was interesting, given previous reports that burn injury increases osteogenic differentiation of wild-type adMSCs [2]. This suggests that burn injury may actually decrease the osteogenic capacity of mesenchymal cells, which may be responsible for HO in *ob/ob* mice.

Diabetes, angiogenesis, and pathologic HO

Hif1 α induces *Vegfa* expression, which directs vessel growth. We noted slightly increased *Hif1 α* transcript and staining in the *ob/ob* mouse hind limb. We also found elevated *Vegfa* transcript and staining in the *ob/ob* hind limb, indicative of robust angiogenic signaling. Our findings were

confirmed by the presence of robust angiogenesis at 7 weeks post-trauma in the *ob/ob* mouse. Therefore, decreased HO volume seen early in leptin-deficient mice is likely not related to decreased angiogenic signaling. Importantly, this difference was not present at baseline when comparing uninjured wild-type and *ob/ob* mice; rather, it appeared that there was a trend toward increased VEGF expression in wild-type mice. We did note that vessels in *ob/ob* mice were narrower and more disorganized. Whether this contributes to diminished HO is difficult to confirm.

Endochondral ossification and leptin deficiency

Normal bone healing occurs through endochondral ossification. During this process, undifferentiated MSCs condense at the site of future bone growth. These MSCs differentiate into chondrocytes, which hypertrophy and produce matrix proteins [23,24]. In this study, we chose to use MSCs derived from the inguinal fat pad to study differences in osteogenic potential between wild-type and *ob/ob* mice. We chose to study these cells as opposed to osteoblasts from wild-type and *ob/ob* mice because we are interested in understanding how leptin deficiency alters osteogenic potential of HO precursor cells and not of mature osteoblasts.

Osteoblasts and vessels invade the surrounding matrix, forming bone. SOX9 is a transcription factor known to play a central role in chondrogenic signaling. Incidentally, *Hif1 α* also regulates SOX9 expression. Although *Hif1 α* levels were elevated in *ob/ob* mice, and there was more downstream proangiogenic signaling (*Vegfa*) in *ob/ob* mice, SOX9 levels were actually diminished in the *ob/ob* mice at both 5 days and 3 weeks after injury. This suggests that *Hif1 α* was unable to induce SOX9 expression with the same efficiency in *ob/ob* mice as in wild-type mice. Pentachrome staining at 3 weeks confirmed diminished cartilage production in the *ob/ob* mouse compared with wild type. These findings strongly suggest that the diminished chondrogenic differentiation contributes to diminished HO as early as 3 weeks post-trauma.

Next, we performed aniline blue and osteocalcin immunofluorescent staining of *ob/ob* and wild-type HO sections at 3 months after trauma. We found that aniline blue staining was much deeper in the wild-type mice for both HO and normal bone compared with the HO or normal bone of *ob/ob* mice. The fact that even normal bone appears to have diminished osteoid in the *ob/ob* mice compared with wild-type mice suggests that the effect of leptin deficiency on normal bone may be similar to its effect on developing HO (Fig. 4). Furthermore, these results are consistent with our pentachrome stain, which showed more red stain indicative of immature collagen deposition. In addition, HO from wild-type mice had more osteocalcin staining on immunofluorescence, suggesting more osteoblast presence within wild-type HO.

Increased osteoclast presence in *ob/ob* mice

Between 7 and 9 weeks, *ob/ob* mice showed decreased ectopic bone volume over time, in stark contrast to wild-type mice. Previous studies demonstrated that osteoclast function is upregulated in the setting of diabetes, prompting our interest in osteoclast presence in our model [12,13].

Osteoclast activity is one mechanism believed to contribute to osteoporosis in diabetic patients. We stained sections of HO in *ob/ob* and wild-type mice with TRAP to assess for osteoclast presence. We noted robust osteoclast presence at 3 weeks in *ob/ob* mice with persistent activity at 11 weeks postinjury. We noted no osteoclast presence in the HO of wild-type mice. This finding suggests a mechanism by which HO is resorbed in the *ob/ob* mouse model of diabetes.

Limitations

In this study, we use leptin-deficient *ob/ob* mice as a model for type 2 diabetes. Serum from *ob/ob* and wild-type mice in our study confirms that the *ob/ob* mice have significantly higher glucose and insulin levels, similar to type 2 diabetes. However, it is also possible that leptin deficiency itself is responsible for decreased HO in the *ob/ob* mouse. To study this, it may be required to determine whether leptin deficiency is sufficient to decrease HO in the absence of hyperglycemia or hyperinsulinemia. Previously, it has been shown that *ob/ob* mice without hyperglycemia have a very low rate of bony turnover.

Conclusions

We demonstrate that pathologic bone formation after trauma, or HO, is limited in the setting of diabetes. Our study using the *ob/ob* mouse model suggests that this may be secondary to impaired early SOX9 activation and chondrogenic differentiation, followed by late bone resorption by osteoclasts. Diabetic mouse models serve as a promising tool to study targets for the prevention or treatment of HO.

Acknowledgments

The authors thank the Department of Radiology at The University of Michigan for the use of The Center for Molecular Imaging and the Tumor Imaging Core, which are supported, in part, by the NIH grant P30 CA046592. B.L. received funding from NIH/NIGMS-K08GM109105-0, Plastic Surgery Foundation National Endowment Award, the Association for Academic Surgery Roslyn Award and the Research & Education Foundation Scholarship, American Association for the Surgery of Trauma Research & Education Foundation Scholarship, DOD: W81XWH-14-DMRDP-CRMRP-NMSIRA, and American Association of Plastic Surgery Research. S.A. funded by the NIH LRP and Collier Society. S.L. funded by HHMI fellowship.

Author Disclosure Statement

No competing financial interests exist.

References

- Potter BK, JA Forsberg, TA Davis, KN Evans, JS Hawksworth, D Tadaki, TS Brown, NJ Crane, TC Burns, FP O'Brien and EA Elster. (2010). Heterotopic ossification following combat-related trauma. *J Bone Joint Surg Am* 92(Suppl 2):74–89.
- Peterson JR, S De La Rosa, H Sun, O Eboda, KE Cilwa, A Donneys, M Morris, SR Buchman, PS Cederna, et al. (2014). Burn injury enhances bone formation in heterotopic ossification model. *Ann Surg* 259:993–998.
- Forsberg JA and BK Potter. (2010). Heterotopic ossification in wartime wounds. *J Surg Orthop Adv* 19:54–61.
- Lin L, Q Shen, T Xue and C Yu. (2010). Heterotopic ossification induced by Achilles tenotomy via endochondral bone formation: expression of bone and cartilage related genes. *Bone* 46:425–431.
- Tannous O, AC Stall, C Griffith, CT Donaldson, RJ Castellani, Jr., and VD Pellegrini, Jr. (2013). Heterotopic bone formation about the hip undergoes endochondral ossification: a rabbit model. *Clin Orthop Relat Res* 471:1584–1592.
- Raghu P, T Dornan, B Dye and JP Palmer. (1983). Diabetes mellitus and skeletal fracture. *JAMA* 249:353.
- Mascitelli L and F Pezzetta. (2006). Type 2 diabetes and fracture risk. *Lancet* 368:732.
- Macey LR, SM Kana, S Jingushi, RM Terek, J Borretos and ME Bolander. (1989). Defects of early fracture-healing in experimental diabetes. *J Bone Joint Surg Am* 71:722–733.
- Turner RT, KA Philbrick, CP Wong, DA Olson, AJ Branscum and UT Iwaniec. (2014). Morbid obesity attenuates the skeletal abnormalities associated with leptin deficiency in mice. *J Endocrinol* 223:M1–M15.
- Turner RT, SP Kalra, CP Wong, KA Philbrick, LB Lindenmaier, S Boghossian and UT Iwaniec. (2013). Peripheral leptin regulates bone formation. *J Bone Miner Res* 28:22–34.
- Tsai TL, PA Manner and WJ Li. (2013). Regulation of mesenchymal stem cell chondrogenesis by glucose through protein kinase C/transforming growth factor signaling. *Osteoarthritis Cartilage* 21:368–376.
- Dienelt A and NI zur Nieden. (2011). Hyperglycemia impairs skeletogenesis from embryonic stem cells by affecting osteoblast and osteoclast differentiation. *Stem Cells Dev* 20:465–474.
- Catalfamo DL, TM Britten, DL Storch, NL Calderon, HL Sorenson and SM Wallet. (2013). Hyperglycemia induced and intrinsic alterations in type 2 diabetes-derived osteoclast function. *Oral Dis* 19:303–312.
- Peterson JR, S De La Rosa, O Eboda, KE Cilwa, S Agarwal, SR Buchman, PS Cederna, C Xi, MD Morris, et al. (2014). Treatment of heterotopic ossification through remote ATP hydrolysis. *Sci Trans Med* 6:255ra132.
- Coleman DL. (1982). Diabetes-obesity syndromes in mice. *Diabetes* 31:1–6.
- Drel VR, N Mashtalir, O Ilnytska, J Shin, F Li, VV Lyzogubov and IG Obrosova. (2006). The leptin-deficient (*ob/ob*) mouse: a new animal model of peripheral neuropathy of type 2 diabetes and obesity. *Diabetes* 55:3335–3343.
- Levi B, ER Nelson, K Brown, AW James, D Xu, R Dunlevie, JC Wu, M Lee, B Wu, et al. (2011). Differences in osteogenic differentiation of adipose-derived stromal cells from murine, canine, and human sources in vitro and in vivo. *Plast Reconstr Surg* 128:373–386.
- Peterson JR, PI Okagbare, S De La Rosa, KE Cilwa, JE Perosky, ON Eboda, A Donneys, GL Su, SR Buchman, et al. (2013). Early detection of burn induced heterotopic ossification using transcutaneous Raman spectroscopy. *Bone* 54:28–34.
- Yin GN, JK Ryu, MH Kwon, SH Shin, HR Jin, KM Song, MJ Choi, DY Kang, WJ Kim and JK Suh. (2012). Matrigel-based sprouting endothelial cell culture system from mouse corpus cavernosum is potentially useful for the study of endothelial and erectile dysfunction related to high-glucose exposure. *J Sex Med* 9:1760–1772.

20. Donneys A, DM Weiss, SS Deshpande, S Ahsan, CN Tchanque-Fossuo, D Sarhaddi, B Levi, SA Goldstein and SR Buchman. (2013). Localized deferoxamine injection augments vascularity and improves bony union in pathologic fracture healing after radiotherapy. *Bone* 52:318–325.
21. Levi B, JS Hyun, ER Nelson, S Li, DT Montoro, DC Wan, FJ Jia, JC Glotzbach, AW James, et al. (2011). Non-integrating knockdown and customized scaffold design enhances human adipose-derived stem cells in skeletal repair. *Stem Cells* 29:2018–2029.
22. Seitz O, C Schurmann, N Hermes, E Muller, J Pfeilschifter, S Frank and I Goren. (2010). Wound healing in mice with high-fat diet- or ob gene-induced diabetes-obesity syndromes: a comparative study. *Exp Diabetes Res* 2010:476969.
23. Mackie EJ, L Tatarczuch and M Mirams. (2011). The skeleton: a multi-functional complex organ: the growth plate chondrocyte and endochondral ossification. *J Endocrinol* 211:109–121.
24. Mackie EJ, YA Ahmed, L Tatarczuch, KS Chen and M Mirams. (2008). Endochondral ossification: how cartilage is converted into bone in the developing skeleton. *Int J Biochem Cell Biol* 40:46–62.

Address correspondence to:

Dr. Benjamin Levi

Department of Surgery

University of Michigan Health System

1500 East Medical Center Drive

2130 Taubman Center SPC 5340

Ann Arbor, MI 48109-0219

E-mail: blevi@umich.edu

Received for publication April 10, 2015

Accepted after revision August 29, 2015

Republished on Liebert Instant Online September 28, 2015

This article has been cited by:

1. Huaqi Jiang, Yuhui Chen, Guorong Chen, Xingguo Tian, Jiajun Tang, Lei Luo, Minjun Huang, Bin Yan, Xiang Ao, Wen Zhou, Liping Wang, Xiaochun Bai, Zhongmin Zhang, Liang Wang, Cory J. Xian. 2018. Leptin accelerates the pathogenesis of heterotopic ossification in rat tendon tissues via mTORC1 signaling. *Journal of Cellular Physiology* **233**:2, 1017-1028. [[Crossref](#)]
2. Carina Cristina Montalvany-Antonucci, Marina C. Zicker, Marina C. Oliveira, Soraia Macari, Mila Fernandes M. Madeira, Ildeu Andrade, Adaliene Versiani M. Ferreira, Tarcilia A. Silva. 2018. Diet versus jaw bones: Lessons from experimental models and potential clinical implications. *Nutrition* **45**, 59-67. [[Crossref](#)]
3. Jeffrey C. Schneider, Laura C. Simko, Richard Goldstein, Vivian L. Shie, Betty Chernack, Benjamin Levi, Prakash Jayakumar, Karen J. Kowalske, David N. Herndon, Nicole S. Gibran, Colleen M. Ryan. 2017. Predicting Heterotopic Ossification Early After Burn Injuries. *Annals of Surgery* **266**:1, 179-184. [[Crossref](#)]
4. Yuqi Guo, Chengzhi Xie, Xiyan Li, Jian Yang, Tao Yu, Ruohan Zhang, Tianqing Zhang, Deepak Saxena, Michael Snyder, Yingjie Wu, Xin Li. 2017. Succinate and its G-protein-coupled receptor stimulates osteoclastogenesis. *Nature Communications* **8**, 15621. [[Crossref](#)]
5. Rhys D. Brady, Sandy R. Shultz, Stuart J. McDonald, Terence J. O'Brien. 2017. Neurological heterotopic ossification: Current understanding and future directions. *Bone* . [[Crossref](#)]